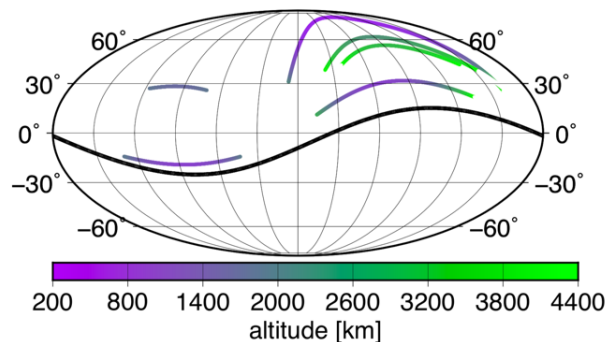


**REGIONAL POWER SPECTRAL ESTIMATION WITH APPLICATION TO GALILEO DATA OF GANYMEDE.** A. C. Mills<sup>1</sup> and A. M. Plattner<sup>1</sup>, <sup>1</sup>Department of Geological Sciences, University of Alabama, Tuscaloosa, AL, USA (acmills1@crimson.ua.edu)

**Background:**

From 1996-2001, the Galileo spacecraft completed 8 flybys of Ganymede, Jupiter's largest moon. Galileo magnetometer data allowed [1] to discover that Ganymede possesses an internal magnetic field, interpreted to stem from a dynamo [1; 2; 3; and 4]. Studies of Ganymede's internal magnetic field are restricted by the limited coverage of Galileo's tracks and their wide altitude range (**Fig. 1**).



**Fig. 1.** Galileo flybys within Ganymede's magnetosphere (identified as shown in **Fig. 2**) above the mean radius of 2634 km. The black line represents the spherical cap for which we intend to calculate a regional power spectrum.

Ganymede's orbit lies within Jupiter's magnetosphere. As a consequence, Ganymede is shielded from solar wind. Plasma within Jupiter's magnetosphere leads to an interaction with Ganymede's magnetic field, creating a magnetopause and a magnetotail. As a consequence, the plasma within Jupiter's magnetosphere limits the distance from which we can observe Ganymede's internal field (**Fig. 2**).

To identify the time stamps when the spacecraft entered and exited Ganymede's magnetosphere, we followed the approach of [8]. As did [8], we observed a change in magnetic field direction and an increase in high-frequency variations when the satellite entered and exited the planetary body's magnetosphere. In **Fig. 2**, we show these time stamps as dashed vertical lines. To reduce the influence of magnetopause and magnetotail fields on the data, we only use data collected a few seconds into the magnetosphere, as indicated by the dash-dotted lines in **Fig. 2**.

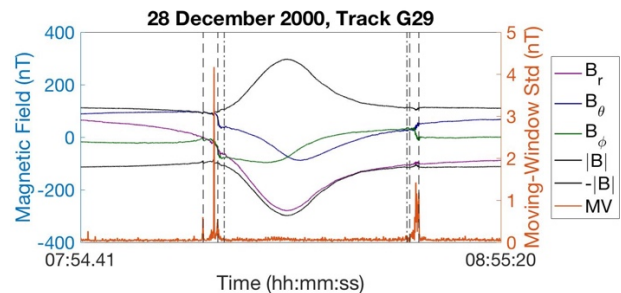


**Fig. 2.** Galileo magnetometer data for G29 transit on December 28, 2000 in the Ganymede-centered planetocentric right-handed (GSPRH) coordinate system:  $r$  (purple),  $\theta$  (green),  $\phi$  (blue), and the magnitude (black). Vertical dashed lines represent the crossing times into and out of Ganymede's magnetosphere. The moving-window standard deviation (orange) is used to identify the magnetosphere. Time is in 24 hour format.

Magnetic field power per spatial length scale, called the spherical-harmonic power spectrum, can be useful to study a range of aspects of an internal magnetic field including source depth and type of dynamo [9; 10; 11; 12; and 13]. While the data coverage of Ganymede does not allow us to determine the full power spectrum, regional approaches [14 and 15] can provide us with a local version of the power spectrum.

We intend to invert for Ganymede's regional power spectrum, directly from the raw data, for the spherical cap of opening angle  $95^\circ$ , centered at longitude  $100^\circ$  and latitude  $20^\circ$  as shown in **Fig. 1**.

**Method:**

Here we adapt the approach of [14 and 15] to directly calculate a regional version of the Mauersberger-Lowes power spectrum [16; 17; and 18] from the raw data. As did [15], we calculate a regional power spectrum by tapering the magnetic field  $d(\mathbf{r})$  through multiplication with a tapering function  $g_\alpha(\mathbf{r})$ .

$$\hat{S}_l^\alpha = (l + 1) \sum_{m=-l}^l \left| \int_{\Omega} g_\alpha(\mathbf{r}) d(\mathbf{r}) Y_{lm}(\mathbf{r}) d\Omega \right|^2 \quad (1)$$

Here,  $Y_{lm}$  is the fully normalized spherical-harmonic function for degree  $l$  and order  $m$ . To minimize the variance of the regional spectrum, we calculate regional power spectra  $\hat{S}_l^\alpha$  using  $N$  different tapering functions,  $g_\alpha$  for  $\alpha=1, \dots, N$ , and average these using weights  $\gamma_\alpha$  for  $\alpha=1, \dots, N$ , that depend on the spatial concentration of the tapering function. Multiplication in the spatial

domain is convolution in the spectral domain. Hence, we want our tapering functions to be as bandlimited as possible while focusing on the spatial region of data availability. The scalar Slepian functions [19] are ideal candidates for such tapering functions.

$$\hat{S}_l = \sum_{\alpha=1}^N \gamma_{\alpha} \hat{S}_l^{\alpha} \quad (2)$$

To calculate regional power spectra directly from the raw data, we replaced the integral in equation (1) with a least-squares inversion for the spherical-harmonic coefficients of the product of the recorded magnetic field radial component with the tapering functions. We obtain the Mauersberger-Lowes spectrum from the radial-field spectrum through degree-wise division by  $(l+1)^2$ , see [16]

Our method directly obtains a power spectrum from raw data without first inverting for the spherical-harmonic coefficients of the magnetic field on the planet's surface. An alternative approach would be to first invert for spherical-harmonic coefficients using a regional approach (e.g. [20]) and then obtaining the regional power spectrum from the spherical-harmonic coefficients. We compare the two approaches in Fig. 3 for synthetic data created from the CHAOS-6 model [21] of Earth's magnetic field. The black line shows the regionalized power spectrum obtained by multiplication of the CHAOS-6 power spectrum with a coupling matrix for Slepian functions with spherical-harmonic bandlimit 2 [see 14 and 15]. The purple lines show the regional spectral results using the method presented here for a range of regularization parameters. The green lines show the results when first inverting for a regional model using a similar range of regularization parameters, and then calculating the regional power spectrum. Regional spectra obtained by direct calculation have a higher fidelity and a smaller variance than when we first invert for a regional model and then calculate the spectrum. Neither method perfectly fits the original power spectrum for the lowest and highest spherical-harmonic degrees, because of the limited data coverage (northern hemisphere only) and random noise that we had added to the synthetic data.

Regional data availability typically leads to biased power spectra [14 and 15]. Our goal is to take this bias into account when calculating and interpreting a power spectrum for Ganymede's magnetic field by following the regional power spectral approach by [14] and [15].

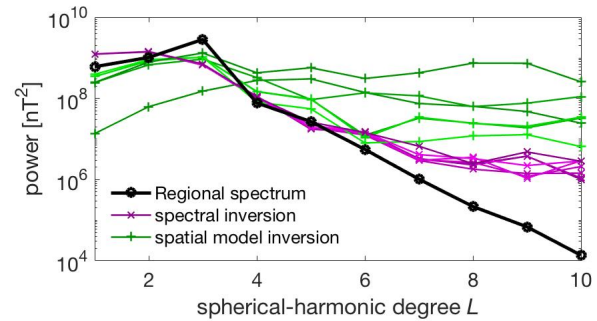


**Fig. 3.** Comparison of directly calculating the regional power spectrum (purple lines) with the alternative method of first inverting for a regional model and then calculating the power spectrum (green lines) from random data locations in the northern hemisphere. Black line is the regionalized global power spectrum for Earth

**Acknowledgments:** The GO-J-MAG-3-RDR-HIGHRES-V1.0 bundle set was obtained from the Planetary Data System (PDS). We thank C. L. Johnson for help with identifying the magnetopause and magnetotail in the flyby tracks. Matlab codes are available from <https://github.com/Slepian/Slepian>.

#### References:

- [1] Kivelson, M.G. et al. (1996) *Letters to Nature*, 384, 537-541. [2] Kivelson, M.G. et al. (1997) *Geophys. Res. Lett.*, 103, 19963-19972. [3] Kivelson, M.G. et al. (2000) *Science*, 289, 1340-1343. [4] Bland, M.T. et al. (2008) *Icarus*, 198, 384-399. [5] Kivelson, M.G. et al. (1997) *Geophys. Res. Lett.*, 24, 2155-2158. [6] Kivelson, M.G. (2007) *The Encyclopedia of the Solar System*, 519. [7] Jia, X. et al. (2006) *COSPAR Scientific Assembly XXXVI*, Abstract # 1479. [8] Winslow et al. (2015) *J. Geophys. Res. Space Phys.*, 118, 2213- 2227. [9] Purucker, M.E. and Whaler, K.A. (2007) *Treatise of Geophysics*, 197-226. [10] Voorhies, C.V. et al. (2002) *J. Geophys. Res.*, 107, E6, 5034. [11] Langlais, B. et al. (2014) *Earth Planet. Sc. Lett.*, 401, 347-358. [12] Wicczorek, M.A. (2018) *J. Geophys. Res. Planets*, 123, 1. [13] Zhan, X. and Schubert, G. (2012) *J. Geophys. Res.*, 117. [14] Wicczorek, M.A. and Simons, F.J. (2005) *Geophys. J. Int.*, 162, 655-675. [15] Dahlen, F.A. and Simons, F.J. (2008) *J. Geophys. Lett. Geodesy*, 174, 774-807. [16] Lowes, F.J. (1966) *J. Geophys. Res.*, 71, 2179. [17] Mauersberger, P. (1956) *Gerlands Beitr. Geophys.*, 65, 207-215. [18] Lowes, F.J. (1974) *J. Geophys. Res.*, 36, 717. [19] Simons, F.J. and Dahlen, F.A. (2006) *Geophys. J. Int.*, 166, 3, 1039-1061. [20] Plattner, A.M. and Simons, F.G. (2017) *Geophys. J. Int.*, 211, 207-238. [21] Finlay, C.C. et al. (2006) *Earth, Planets, and Space*, 68, 112.